

## COMBUSTION OF INTERACTING DROPLET ARRAYS IN A MICROGRAVITY ENVIRONMENT

Daniel L. Dietrich  
NASA Lewis Research Center, Cleveland, Ohio 44135

### Introduction

This research program involves the study of one and two dimensional arrays of droplets in a buoyant-free environment. The purpose of the work is to extend the database and theories that exist for single droplets into the regime where droplet interactions are important. The eventual goal being to use the results of this work as inputs to models on spray combustion where droplets seldom burn individually; instead the combustion history of a droplet is strongly influenced by the presence of the neighboring droplets.

Throughout the course of the work, a number of related aspects of isolated droplet combustion have also been investigated. This paper will review our progress in microgravity droplet array combustion, advanced diagnostics (specifically LII) applied to isolated droplet combustion, and radiative extinction large droplet flames. A small-scale droplet combustion experiment being developed for the Space Shuttle will also be described.

Droplet Array Combustion (with Kunihiro Kitano and Senji Honma, Hokkaido National Industrial Research Institute, Sapporo, JAPAN)

Recently, Annamali and Ryan [1] have summarized the current status of droplet array, cloud and spray combustion. A number of simplified theories [2-8], and detailed numerical studies [9,10] of droplet vaporization/combustion where multiple droplet effects are present are now available. These theories all neglect the effect of buoyancy. Experimentally, most studies to date suffer the effects of buoyancy is; it becomes the dominant transport mechanism in the problem. Only the works of Law and co-workers [11,12] and more recently by Mikami *et al.* [13] were performed in an environment where buoyancy effects were small. Law and co-workers were limited to high oxygen index, low pressure ambient environments since there studies were conducted in normal gravity.

Studies are now being conducted in normal and microgravity involving interacting droplet arrays in sealed chambers, where the ambient can be controlled. Droplets are typically suspended on 125  $\mu\text{m}$  optical fibers with small ( $\sim 250 \mu\text{m}$ ) beads on the end. A coiled hot-wire ignites the droplet, and then is removed immediately. Backlit images provide droplet diameter-time history and an orthogonol view provides flame-diameter time history. Recently Mikami *et al.* [13] showed that droplet arrays burning in microgravity do not burn in accordance with the d-squared law. The burning rates discussed below nonetheless are obtained by a linear least squares fit of the data.

Figure 1 shows results from a three-droplet array burning in air in microgravity. The fuel was n-heptane with initial droplet sizes of approximately 1.4 mm. Figure 1a (left) shows the burning history of each droplet in the array for  $L/D = 7.1$ , and Figure 1b (right) shows the burning history

of the center droplet of the array for different L/D's. Figure 1a shows that the center droplet in the array had the slowest burning rate of the three droplets. Figure 1b shows that a single n-heptane droplet has the largest burning rate. The burning rate then continuously decreases as the inter-droplet separation distance decreases.

In normal gravity tests, a horizontal two-droplet array of n-decane burning in air at 1 atm shows just the opposite behavior. The burning rate increases due to droplet interactions. For instance, the burning rate of a single n-decane droplet is  $1.0 \text{ mm}^2/\text{s}$ , but for a two droplet array with an initial, normalized (L/D) inter-separation distance of 4 the burning rate increases slightly to  $1.1 \text{ mm}^2/\text{s}$ .

In normal gravity, oxygen transport is enhanced by buoyant convection. In this case, the neighboring droplets reduce the heat loss during burning, and the burning rate increases. In microgravity, the buoyant heat loss is greatly reduced but so is the oxygen transport rate to the flame. In this case, the droplets actually compete with each other for oxygen. The burning rate, thus decreases. The center droplet, which is surrounded by other droplets receives the least amount of oxygen even though this droplet has the minimum heat loss. The burning rate of the center droplet is thus smaller than the other two. Symmetry dictates that the left and right droplets should have the identical burning rates, as is verified by the experimental data.

#### Isolated Droplet Combustion (with R. Vander Wal, NYMA, Inc.)

Traditionally, the diagnostics used on droplet combustion studies (especially in microgravity) have been limited to orthogonal views of the flame and droplet. While backlighting provides simple and accurate measurements of the droplet size (assuming proper adjustment of the light source and imaging system), simple pictures of the flame do not always provide accurate information. There are ambiguities regarding exactly what is being visualized, including the fact that a two-dimensional image of a three dimensional object is formed. Also, with the increasing use of video cameras, experimental results show that the observed size of the flame can vary as a function of camera gain, with large errors if saturation occurs. Since there is a range of colors and intensities in a droplet flame, it is difficult to select a single gain which is appropriate for the entire flame.

Studies in normal gravity have been conducted to try to gain an understanding of how the visible flame compares with different types of measurements. The most significant comparison has been with Laser-Induced Incandescence (LII) which measures the absolute and relative soot volume fraction during droplet combustion. Simultaneous LII and natural flame, simultaneous LII and OH chemiluminescence, and simultaneous droplet size history, natural flame and radiometric measurements of the flame studies have all been conducted. Although not simultaneously, backlit droplet size histories, which are quite reproducible, have been obtained for all of the fuels in the identical configurations to those above. An example of some of the data collected is given below.

These studies were conducted in a sealed chamber in air at 1 atm. The droplets were suspended by fibers with diameters of 125, 230 and 500  $\mu\text{m}$  with beads on the end with diameters of 250, 400, and 1000  $\mu\text{m}$  respectively. The initial droplet sizes for the three fibers were 1.2, 1.5 and 3 mm, respectively. The ignition system for the smaller droplets was a length of 250  $\mu\text{m}$  Kanthal (Aluminum alloy) wire heated with a current of approximately 3 amps, that was removed immediately after ignition. The ignition system for the tests using the largest fiber and bead was a spark. The droplet dispense, deployment, and ignition systems were controlled by a portable computer which also provided a trigger pulse for the data acquisition system (LII). The fuels used in the tests were selected to show a wide range of sooting tendencies, heptane, decane (commonly used fuels), chloroheptane and chlorodecane.

A description and characterization of the two-dimensional LII system are described elsewhere [14,15, also presented at this workshop]. Both natural flame images and OH chemiluminescence images were taken with a second gated, intensified camera synchronized with the LII camera. For the largest droplet studies, the intensified array camera was used to capture backlit views of the droplet, but for all others, either black and white or color CCD cameras connected to a long working-distance microscope were used.

Figure 2 shows representative burning histories for each of the fuels, along with the least squares fit burning rate constants. Also shown are the relative average soot volume fractions for the produced for the two fuels [completely described in 15,16]. All of the tests were conducted in normal gravity with a 1 atm, air ambient. As the droplet hangs on the fiber, it is not spherical, but elongated. The equivalent droplet diameter plotted in Fig 2 was computed by three different methods, two from the volume and surface area equivalent diameter of an ellipsoid, and another from the projected area of the droplet. All methods produced equivalent droplet diameters and burning rate constants that were within a few percent of each other. Figure 3 shows both natural flame and LII images of n-decane and 1-chlorodecane.

Figure 2 shows that the burning rate constants for the heptane and decane are nearly identical, as expected. The burning rate constants for the chloroheptane and chlorodecane are also nearly equal to each other and to the value obtained for heptane and decane (within 12 percent). As seen in the table of Figure 2, the relative soot production from the fuels, however, is dramatically different.

The LII results show that, relative to heptane, decane has soot volume fractions twice that of heptane. The visible structure of the two flames, however, is nearly identical. Both are blue at the base or bottom and yellow near the top. The flame sizes (relative to the droplet) are also similar for the two fuels. The chlorinated fuels produce average soot volume fractions more than an order of magnitude larger than that of heptane. The structure of the flames is very different also. Both chlorinated fuels are open-tipped at the top, with significant soot escape. No soot was present at the bottom of the flame for the chlorinated fuels and the flame was blue there.

The fact that the burning rates were identical but the soot production varied so much can be explained as follows. The vaporization of the droplet is controlled by the heat feedback to the droplet. In normal gravity, the soot production occurs downstream of the droplet and the heat produced here does not significantly the vaporization rate of the fuel. Instead, the vaporization is controlled by the flame close to the bottom of the droplet.

#### Radiation Losses in Large Droplet Burning (with P. Struk, GSRP, and J.S. T'ien, CWRU)

Radiative losses in droplet burning are usually neglected in theoretical and numerical treatments of droplet burning. The limitingly small droplet diameter below which a spherical flame cannot exist is well documented and is a topic of a space flight microgravity investigation (DCE). A recent theoretical treatment by Chao et al. [17] shows that for a droplet burning with spherical symmetry, there will be a *large* droplet size above which a flame will not exist. The mechanism for the existence of this limit is radiative extinction.

Some preliminary experimental evidence was obtained in the JAMIC facility for the burning of a large (3-4 mm) decane droplet. Immediately after ignition the flame was as expected, bright yellow, sooty and spherical (except for a small non-uniformity due to a small convective flow). As the burning progressed, the luminosity of the flame decreased, and by the end of the drop, the droplet had not yet burned to completion, and the flame was nearly invisible to the CCD camera. While the flame was barely visible by the end of the test, it also did not extinguish. In a subsequent test, a smaller (1-2 mm initial diameter) n-decane droplet burned to completion as expected, with a bright yellow, sooty, spherically symmetric flame.

Further testing and analysis is required before any conclusions can be drawn from this preliminary data. This could be an indication, however, of increased radiative heat transfer cooling the flame such that less soot is produced. On the other hand, since these were the first tests in a new experimental apparatus, there could have been some experimental problem that caused this unusual result.

The radiative extinction phenomena for droplets is most easily observed in reduced gravity, where a droplet can burn with spherical symmetry and convective losses are minimized. To further study this problem, steady-state droplet combustion is simulated using a porous sphere which is continually fed with liquid. The liquid flowrate is controlled by a computer operated syringe pump that allows precise control of the flowrate. Initial work in normal gravity has been conducted at reduced pressure ambients. The chamber was the same one described in the previous section. The flowrate of the fuel was adjusted until a steady wetted surface was observed on the porous sphere. Because the chamber was sealed, the burning rate decreased slightly throughout the flame lifetime as a result of the continuously decreasing ambient oxygen concentration. An equivalent burning rate constant was computed as  $k = [4Q/(\pi D)]$  where  $Q$  is the volumetric flowrate and  $D$  is the sphere diameter. The burning rate constant calculated this way is considered valid only when a steady wetted surface is observed.

For n-decane fuel, and a 4 mm diameter bronze sphere, steady burning was achieved at 1/3 atm. The equivalent burning rate constant was approximately 1.2 mm<sup>2</sup>/s. This is higher than the 0.9 mm<sup>2</sup>/s observed for 1.3 mm initial diameter fiber-supported droplets burned in the same facility. The difference is probably due to increased buoyancy effects at the larger droplet sizes with the porous sphere. Visibly, except for the scale factor, the flames from the fiber supported droplets and the porous sphere looked nearly identical; the only difference being that the flame was quenched at the base in the vicinity of the fuel supply tube in the case of the porous sphere.

The droplet diameter can be changed by varying the size of the porous sphere. In reduced gravity, small changes in droplet diameter may be obtained by changing the thickness of liquid film on the surface of the sphere. An experimental apparatus is currently being built which will be flown in the NASA LeRC DC-9 in the near future.

Glovebox Experiment (with F.A. Williams, UCSD; F.L. Dryer, Princeton; B.D. Shaw, UCD; M. Vedha-Nayagam, Analex; J.B. Haggard, NASA LeRC)

Currently manifested on STS-73, the Second United States Microgravity Laboratory (USML-2), is a small-scale droplet combustion experiment called the Fiber-Supported Droplet Combustion (FSDC) experiment. The FSDC is a multi-user facility that supports a wide range of experiments. Single droplets and droplet arrays will be suspended and burned on 80 and/or 150  $\mu$ m Si-C fibers. The droplets are ignited by a coiled hot-wire that withdraws immediately after ignition. The unit is also capable of imparting a uniform, sub-buoyant forced flow (0 - 20 cm/s) on the droplet. The data is derived from a backlit microscope image of the droplet, and an orthogonal view (by either a black and white or color CCD camera) of the flame. Simultaneous 3-axis acceleration measurements will also be made.

This experiment, like all glovebox efforts, is very crew-intensive. The crew sets up the microscope and flame view cameras. The crew also manually dispenses a droplet from a modified syringe(s) onto the fiber and controls the ignition process. The current test matrix will include the combustion of droplets with 3 to 5 mm initial diameter, although smaller droplets can also be burned. Two pure fuels, heptane and methanol (in support of the Droplet Combustion Experiment) will be burned; heptane will also be studied with a forced flow. Fuel mixtures of methanol/dodecanol, methanol/water and heptane/hexadecane will be studied. Finally, several tests of a three-droplet array of pure methanol will be studied.

## Future Work

The porous sphere droplet experiment requires a long-duration reduced gravity environment to observe radiative extinction. The small (2.2 second) drop tower is not suitable for this experiment. The apparatus is currently being modified for use on the DC-9 to see if the aircraft g-levels and duration are sufficient. An existing experiment package will be modified to include a syringe pump and a porous sphere with the ignition system. The majority of the data will be a view showing the state of the porous sphere and an orthogonal view of the flame. The existing color schlieren system will be used in some tests also.

The FSDC investigation will fly aboard the Space Shuttle Columbia in late September 1995. Since the major data is video, experimental results, with the exception of the acceleration data, will be available immediately. The planned test matrix includes 30 test points, although extra fuel is available if extra crew time becomes available.

## References

1. Annamalai, K. and W. Ryan. "Interactive Processes in Gasification and Combustion. Part I: Liquid Drop Arrays and Clouds," *Progress in Energy and Combustion Science* 18, 1992, 221.
2. Brzustowski, T.A., E.M. Twardus, S. Wojcicki and A. Sobiesiak. "Interaction of Two Burning Fuel Droplets of Arbitrary Size," *AIAA Journal* 17, No. 11, 1979, 1234.
3. Labowsky, M. "A Formalism for Calculating the Evaporation Rates of Rapidly Evaporating Interacting Particles," *Combustion Science and Technology* 18, 1978, 145.
4. Labowsky, M. "Calculation of the Burning Rates of Interacting Fuel Droplets," *Combustion Science and Technology* 22, 1980, 217.
5. Marberry, M., A.K. Ray and K. Leung. "Effect of Multiple Particle Interactions on Burning Droplets," *Combustion and Flame* 57, 1984, 237.
6. Samson, R., D. Bedeaux and J.M. Deutch. "A Simple Model of Fuel Spray Burning II. Linear Droplet Streams," *Combustion and Flame* 31, 1978, 223.
7. Umemura, A., S. Ogawa and O. Nobunori. "Analysis of the Interaction Between Two Burning Droplets," *Combustion and Flame* 41, 1981, 45.
8. Umemura, A. "Interactive Droplet Vaporization and Combustion: Approach from Asymptotics," *Progress in Energy and Combustion Science* 20, 1994, 325.
9. Raju, M.S. and W.A. Sirignano. "Unsteady Navier-Stokes Solution for Two Interacting, Vaporizing Droplets," AIAA-87-0300, AIAA 25th Aerospace Sciences Meeting, Reno, Nevada, 1987.
10. Tal, Reuven and W.A. Sirignano. "Cylindrical Cell Model for the Hydrodynamics of Particle Assemblages at Intermediate Reynolds Numbers," *American Institute of Chemical Engineers Journal* 28, No. 2, 1982, 233.
11. Miyasaka, K. and C.K. Law. "Combustion of Strongly Interacting Linear Droplet Arrays," *Eighteenth Symposium (International) on Combustion* / The Combustion Institute, 1981, 283.
12. Xiong, T.Y., C.K. Law, C.K. and K. Miyasaka. "Interactive Vaporization and Combustion of Binary Droplet Systems," *Twentieth Symposium (International) on Combustion* / The Combustion Institute, 1984, 1781.
13. Mikami, M., Kato, H., Sato, J. and Kono, M. "Interactive Combustion of Two Droplets in Microgravity," to appear in the proceedings of the 25th Symposium (International) on Combustion / The Combustion Institute, 1994.
14. Vander Wal, R.L. and Weiland, K.J. "Laser-Induced Incandescence: Development and Characterization Towards a Measurement of Soot Volume Fraction," *Journal of Applied Physics B* (to appear).
15. Vander Wal, R.L. and Dietrich, D.L. "Laser-Induced Incandescence Applied to Droplet Combustion," *Applied Optics* 34, 6, 1995, 1103.
16. Vander Wal, R.L. and Dietrich, D.L. "Relative Soot Volume Fractions in Droplet Combustion via Laser-Induced Incandescence," Presented at the Fall Meeting of the Eastern States Section of the Combustion Institute, 1994.
17. Chao, B.H., Law, C.K. and T'ien, J.S. "Structure and Extinction of Diffusion Flames with Flame Radiation," *Twenty-Third Symposium (International) on Combustion* / The Combustion Institute 1990, 523.

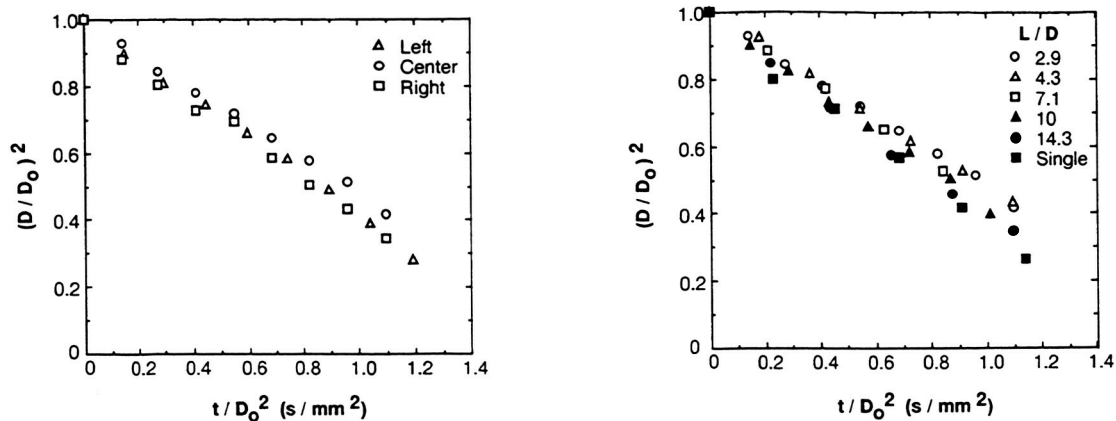


Figure 1. Droplet size histories for a three droplet array of identically sized 1.4 mm initial diameter droplets of n-heptane droplets burning in air.

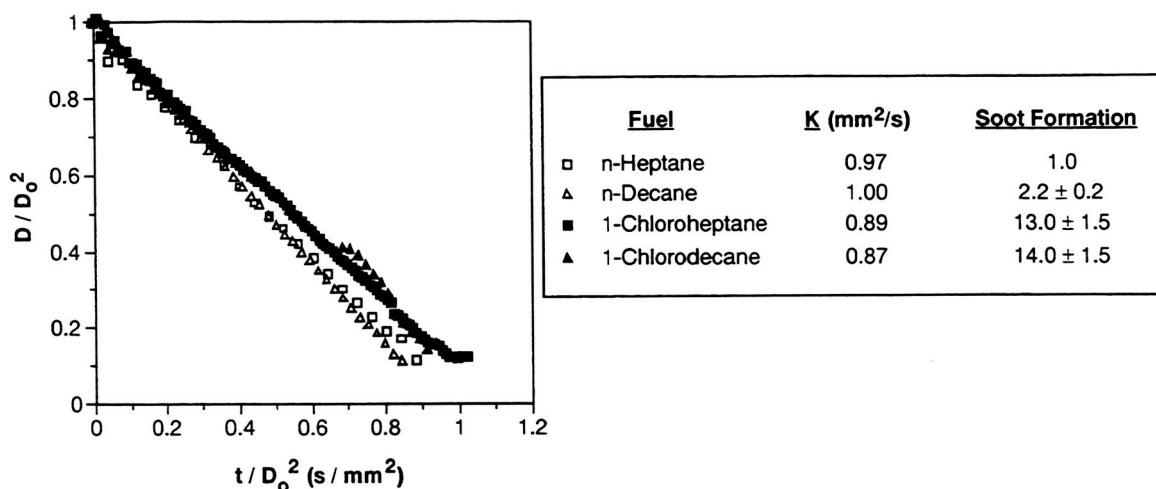


Figure 2. Burning rate constants and relative ammounts of soot formation for four different fuels. The soot formation numbers are relative to heptane.

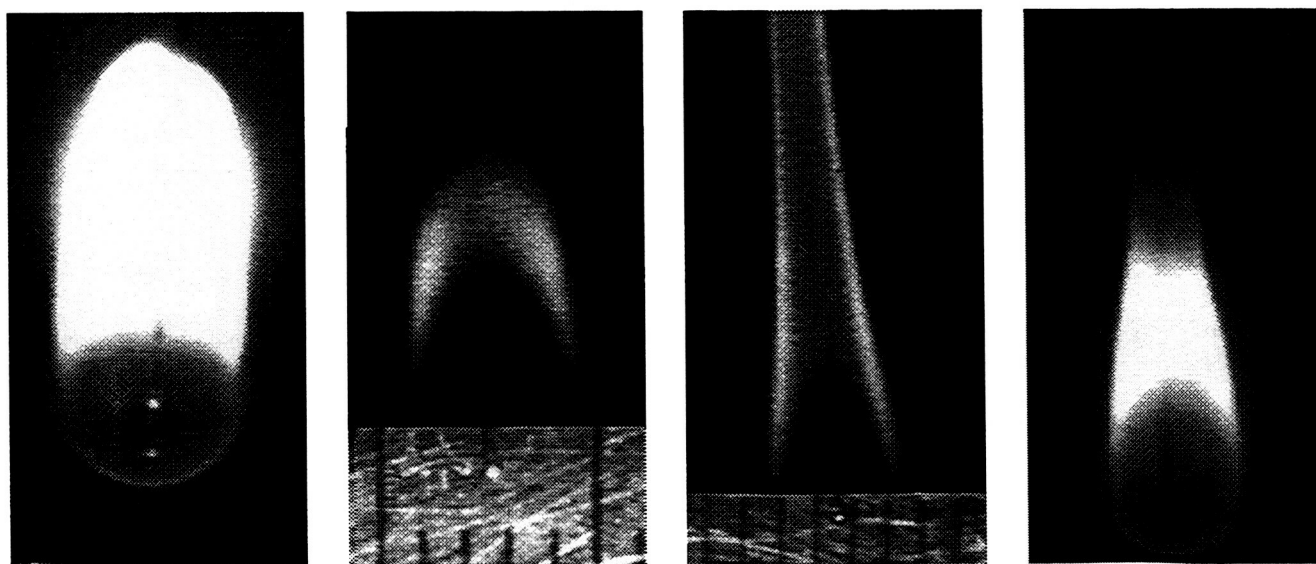


Figure 3. Natural flame (a,c) and LII (b,d) pictures of n-decane (a,b) and chlorodecane (c,d).